

## VISCOELASTIC FLOWS IN 1-TO-4 SUDDEN EXPANSIONS

*G. N. Rocha and P. J. Oliveira\**

<sup>1</sup> Unidade Materiais Têxteis e Papeleiros, Departamento de Engenharia Electromecânica,  
Universidade da Beira Interior, 6201-001 Covilhã, Portugal

\* Corresponding author, Email: pjpo@ubi.pt

Keywords: Planar expansion; Symmetric flow; Viscoelastic fluid; FENE-CR model

### Abstract

In this numerical study we present a systematic investigation of the flow of a FENE-CR liquid in a planar sudden expansion having an area ratio of 1:4. The governing equations are solved with a finite volume method and the interest is confined to steady state solutions in two dimensions. Symmetry about the ducts centre plane is not assumed. In terms of parametric variations, both the Reynolds number, characterising the inertia of the flow, and the Weissenberg number, characterising its viscoelasticity, were varied in a wide range. On the other hand, the extensibility parameter of the FENE-CR model was kept constant, at the value  $L=10$ . The results given comprise flow patterns, vortex size and strength, and pressure and velocity distribution along centreline.

### 1. INTRODUCTION

From a fundamental point of view, viscoelastic fluid flow through ducts with abrupt change of cross section, either expansions or contractions, are important as they highlight many of the unusual phenomena brought about by elasticity. These include complex recirculation patterns, not found with Newtonian fluids, vortex enhancement or suppression, stress behaviour near geometrical singular points, etc. In addition, expansion and contraction geometries are relevant in engineering applications, namely in processing industries, for example the channel feeding an extrusion die is unavoidable endowed with such localised perturbations in cross-section in order to achieve the desired extruded shape. A survey of the specialised literature shows that contraction flows of viscoelastic liquids have received a lot of attention during the past 10-15 years, but studies (both numerical and experimental) of expansion flows are rather scarce.

Examples of this kind of problems we envisage, with both Newtonian and non-Newtonian fluids by Boger and Walters [1]. Numerical studies of sudden expansion flows have been undertaken by Oliveira [2] with viscoelastic fluids and using an expansion ratio 1:3, and by Drikakis [3] with Newtonian fluids and using several expansion ratios. In two-dimensions such studies have established that the size of the recirculating flow region increases linearly with increasing Reynolds number.

While in Newtonian flows the shear stress is proportional to the velocity gradient, non-Newtonian fluids have a shear stress which is not simply proportional solely to the velocity gradient. These fluids may not have a well-defined viscosity and another characteristic is due their viscoelastic properties, making then behaving as either an elastic solid or as a viscous fluid. For laminar flows of Newtonian or non-Newtonian fluids through plane sudden expansions, it is well known that, when the expansion ratio  $E$  exceeds 1.5, the flow field downstream of the expansion becomes asymmetric above a critical Reynolds number. In our case that does not happen because we are here concerned with low Reynolds

number flows and for that reason we do not reach these critical Reynolds numbers. That kind of behaviour is analysed in the articles dealing with numerical simulations of Drikakis (1997) and Oliveira (2003).

Here we present a systematic numerical investigation of the flow of a FENE-CR liquid in a planar sudden expansion having an area ratio of 1:4. The governing equations are solved with a finite volume method and steady state solutions are sought in two dimensions. Symmetry about the ducts centre plane is not assumed. In terms of parametric variations, both the Reynolds number, characterising the inertia of the flow, and the Weissenberg number, characterising its viscoelasticity, were varied in a wide range. On the other hand, the extensibility parameter of the FENE-CR model was kept constant, at the value  $L=10$ . The results given comprise flow patterns, vortex size and strength, and pressure and velocity distribution along centreline.

## 2. CONSERVATION AND CONSTITUTIVE EQUATIONS

In this paper we consider the two-dimensional isothermal flow of an incompressible liquid flowing from a straight channel of height  $d=1$  to a larger channel of height  $D=4$ . The upstream channel has a length of  $L_1=20d$  and the downstream channel a length  $L_2=50d$ , as shown in figure 1. This problem is governed by the usual equations of continuity and motion, which can be written as:

$$\nabla \cdot \mathbf{u} = 0 \quad (1)$$

$$\rho \frac{D\mathbf{u}}{Dt} = -\nabla p + \nabla \cdot \boldsymbol{\tau} \quad (2)$$

where  $\mathbf{u}$  is the velocity vector,  $\rho$  is the fluid density (assumed constant),  $p$  is the pressure,  $\boldsymbol{\tau}$  is the extra stress tensor, and  $D(\ )/Dt = \partial(\ )/\partial t + \mathbf{u} \cdot \nabla(\ )$  is the substantial derivative. For a homogeneous polymeric solution the extra stress is decomposed by the sum of a Newtonian solvent and a polymeric solute ( $\boldsymbol{\tau} = \boldsymbol{\tau}_s + \boldsymbol{\tau}_p$ ). The Newtonian solvent component is expressed in eq. (3), where the solvent viscosity  $\eta_s$  is constant,  $\nabla \mathbf{u}^T$  is the transpose of the velocity gradient, and  $\mathbf{D}$  is the rate-of-strain tensor:

$$\boldsymbol{\tau}_s = \eta_s (\nabla \mathbf{u} + \nabla \mathbf{u}^T) \equiv 2\eta_s \mathbf{D} \quad (3)$$

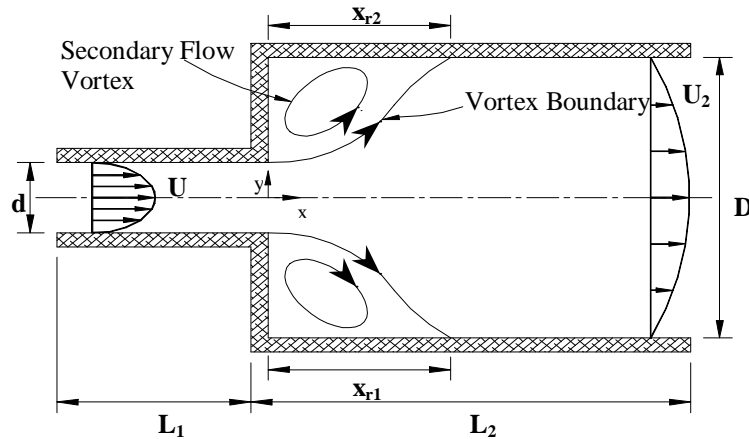


Figure 1- Representation sketch of expansion flow

When the fluid presents simultaneously viscous and elastic properties (a viscoelastic fluid), the problem it is more complicated, compared with the Newtonian case. For solving this problem we use a form of constitutive equation for finite extensibility non-linear dumbbells [4], valid for polymeric materials, proposed by Chilcott and Rallison [5], in which the shear viscosity is constant:

$$\boldsymbol{\tau}_p + \frac{\lambda}{f(\boldsymbol{\tau}_p)} \overset{\nabla}{\boldsymbol{\tau}}_p = 2\eta_p \mathbf{D} \quad (4)$$

with the stretch function  $f(\boldsymbol{\tau}_p)$  expressed by:

$$f(\boldsymbol{\tau}_p) = \frac{L^2 + (\lambda/\eta_p) \text{tr}(\boldsymbol{\tau}_p)}{L^2 - 3} \quad (5)$$

In the previous equations,  $\text{tr}$  is the trace operator,  $\bullet$  is a constant relaxation time,  $\bullet_p$  is the polymer viscosity (constant) and  $L^2$  the extensibility parameter that measures the size of the polymer molecule in relation to its equilibrium size. The symbol  $\overset{\nabla}{\boldsymbol{\tau}}$  in eq. (4) is used to denote Oldroyd's upper convected derivate:

$$\overset{\nabla}{\boldsymbol{\tau}} = \frac{D\boldsymbol{\tau}}{Dt} - \boldsymbol{\tau} \cdot \nabla \mathbf{u} - \nabla \mathbf{u}^T \cdot \boldsymbol{\tau} \quad (6)$$

An additional simplification is embodied in eq. (4), compared with the original FENE-CR equation of Chilcott and Rallison. The modification is to consider  $Df/Dt$  negligible and the new model is denoted FENE-MCR, for modified Chilcott-Rallison model. It has been used, for example, by Oliveira [2]. The following relation clarifies the modification introduced into the model:

$$\left( \overset{\nabla}{f\boldsymbol{\tau}} \right) = f \overset{\nabla}{\boldsymbol{\tau}} + \boldsymbol{\tau} \frac{Df}{Dt} \Leftrightarrow \left( \overset{\nabla}{f\boldsymbol{\tau}} \right) \approx f \overset{\nabla}{\boldsymbol{\tau}} \quad (7)$$

which was useful to facilitate the utilisation of an existing numerical procedure.

The relevant non-dimensional parameters to be varied in this work are the extensibility parameter of the FENE-CR model,  $L^2$ , the solvent viscosity ratio given by:  $\beta = \eta_s / \eta_0$ , where the global shear viscosity is  $\eta_0 = \eta_s + \eta_p$  (constant), the Reynolds number:  $\text{Re} = \rho U d / \eta_0$ , and the Weissenberg number,  $We = \lambda U / d$  where the velocity  $U$  is the average velocity in the smaller channel and  $d$  is the height of that channel.

### 3. NUMERICAL METHOD

In the present study, a finite volume method based on the SIMPLEC algorithm for the pressure-velocity coupling is employed to solve the system of the governing equations using orthogonal meshes. The governing equations (Eqs. (1), (2), (4) and (5)) are integrated in space over the control volumes (cells) forming the computational mesh and are transformed into systems of linearised algebraic equations. This discretisation method and the iterative procedure to solve the large sets of linear equations are explained with more detail in Oliveira et al. [6] and no further description is required here. Suffices to add that a formally third-order accurate scheme, the CUBISTA of ref. [7], is applied to represent the all important convective terms in both the constitutive and the momentum equations.

## 4. RESULTS

At the inlet we have imposed fully developed profiles for all variables, with the velocity profile following a parabolic shape and with an average velocity arbitrarily set to  $U=1$ . For the FENE-MCR model, the fully developed velocity and the shear stress distributions in channel flow are identical to those for a Newtonian fluid. In relation to fig.1, these are:

$$u = 1.5U \left( 1 - \left( \frac{y}{d/2} \right)^2 \right) \text{ and } \tau_{xy} = \eta_p \frac{du}{dy} = - \left( \frac{12\eta_p U}{d} \right) \left( \frac{y}{d} \right) \quad (8)$$

The normal stress  $\sigma_{xx}$  follows a more complicated variation given in ref. [2].

### 4.1. Results for Newtonian case and validation data

In the figures 2 and 3 we compare, respectively, the predicted vortex length ( $X_r = x_r/d$ ) and vortex intensities ( $\bullet_r = \bullet_{r1} = \bullet_{r2}$  in symmetric flow) with existing results, for several Reynolds numbers. For this comparison, we used the correlations proposed by Scott et al. [7] and it can be seen that, for Reynolds numbers above 20, there is good agreement between our predictions and their correlations. Our numerical data are given in Table 2, where a perfect symmetry between the upper ( $y > 0$ ) and lower ( $y < 0$ ) parts of the channel is observed, for the range of Re considered. Recall that we do not rely on the symmetry about the centerplane ( $y = 0$ ), with simulations performed on the full domain.

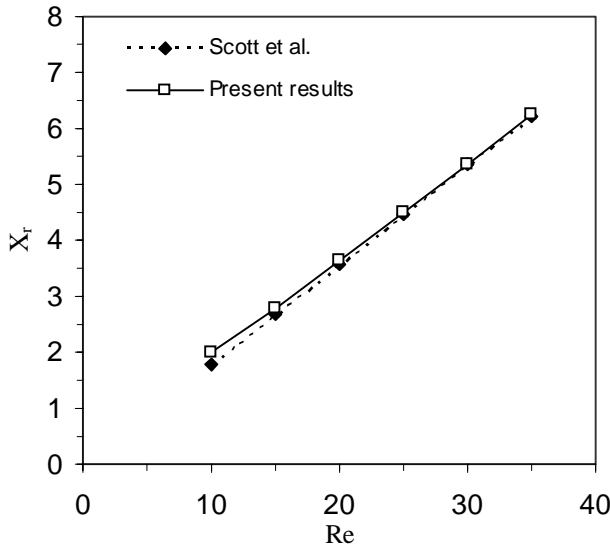


Fig 2 – Vortex length vs Reynolds number

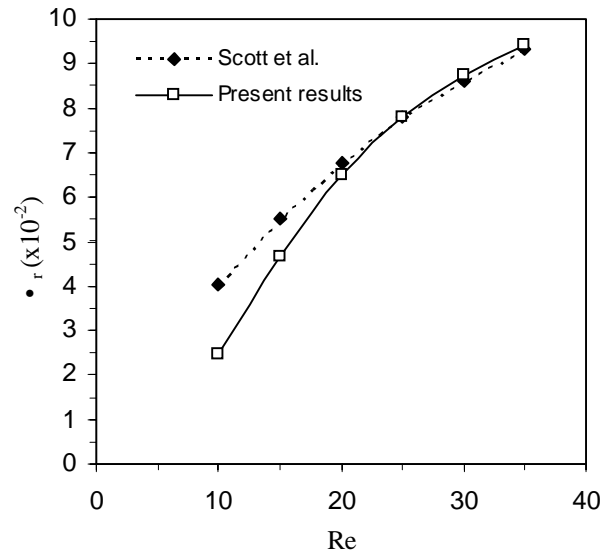


Fig 3 – Vortex intensity vs Reynolds number

Re	$X_{r1}$	$X_{r2}$	$\bullet_{r1} (x10^{-2})$	$\bullet_{r2} (x10^{-2})$
20	3.628	3.628	6.5039	6.5039
15	2.784	2.784	4.6578	4.6578
10	1.989	1.989	2.4580	2.4580
5	1.286	1.286	0.6645	0.6645
2	0.933	0.933	0.1741	0.1741
1	0.831	0.831	0.1029	0.1029
0.1	0.750	0.750	0.0629	0.0629
0.01	0.742	0.742	0.0597	0.0597

Table 2 – Vortex length ( $X_r$ ) and vortex intensity ( $\bullet_r$ ) for Newtonian case

## 4.2. Results for viscoelastic case

For viscoelastic flow, there are four independent parameters in the FENE-MCR model under consideration ( $Re$ ,  $We$ ,  $L^2$  and  $\bullet$ ). In this work, the extensibility parameter was set  $L^2 = 100$  for all simulations and the solvent viscosity ratio  $\bullet$  equal to 0.5; the varying parameters were the Weissenberg number (1; 2; 5), and the Reynolds number, between 0.01 – 20. Table 3 presents some values of vortex size and intensity for the three Weissenberg numbers here considered, at  $Re = 20$ .

We	$X_{r1}$	$X_{r2}$	$\bullet_{r1} (x10^{-2})$	$\bullet_{r2} (x10^{-2})$
1	2.59	2.59	3.556	3.556
2	2.07	2.07	2.231	2.233
5	1.47	1.47	0.851	0.855

Table 3 – Data for the viscoelastic case – effect of Weissenberg number ( $L^2=100$ ,  $\bullet=0.5$ ,  $Re=20$ )

### 4.2.1. Reynolds and Weissenberg numbers dependence

For the higher Reynolds numbers the inertial forces are seen to dominate the flow, whilst for low Reynolds number (less than 1) the viscous forces dominate. The Weissenberg number represents the effect of viscoelasticity on the flow and when  $We$  is small the flow is all slow flow, approach's the Newtonian limit, while for a large  $We$  important elastic effects set in.

In Figures 4 – 9 we present streamlines contour plots for two Reynolds numbers (10 and 20) and for increasing Weissenberg numbers.

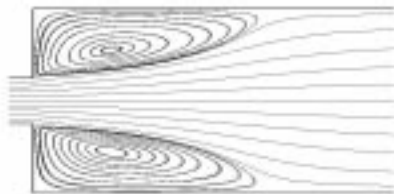


Fig. 4 – Newtonian case with  $Re=20$

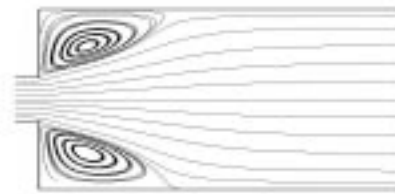


Fig. 5 – Newtonian case with  $Re=10$

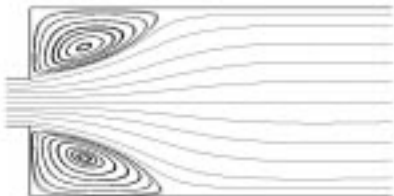


Fig. 6 – Viscoelastic case with  $We = 2$ ,  $Re = 20$

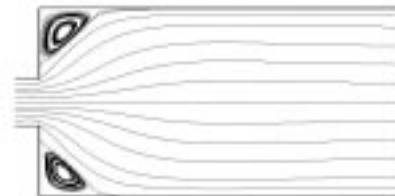


Fig. 7 – Viscoelastic case with  $We = 2$ ,  $Re = 10$

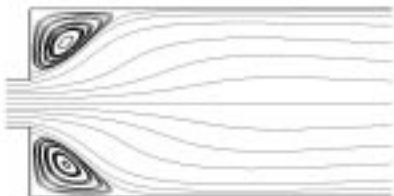


Fig. 8 – Viscoelastic case with  $We = 5$ ,  $Re = 20$

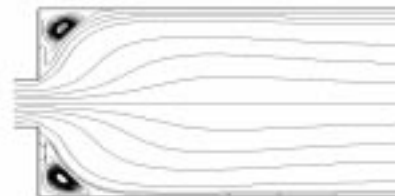


Fig. 9 – Viscoelastic case with  $We = 5$ ,  $Re = 10$

In figure 10 we present, for low Reynolds number ( $Re = 0.01$ ), the variation of the streamwise velocity component along the central plane ( $y = 0$ ), at  $We = 0$  and  $We = 2$  ( $L^2=100$  and  $\bullet=0.5$ ) corresponding to the Newtonian and Viscoelastic cases, respectively. A strong velocity overshoot is observed upstream of the expansion plane, and an undershoot downstream.

In figure 12 we present pressure profiles along the central plane for Newtonian and viscoelastic fluids ( $L^2 = 100$ ,  $\bullet = 0.5$ ,  $We = 2$ ), at  $Re = 20$ . Although not clearly seen, the pressure recovery after the expansion of the Viscoelastic fluid is smaller than for the Newtonian fluid and this leads to a larger localised loss coefficient, in agreement with the findings of [2].

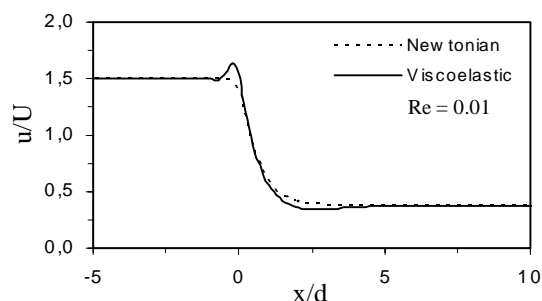


Fig. 10 – Variation of streamwise velocity along the central plane.

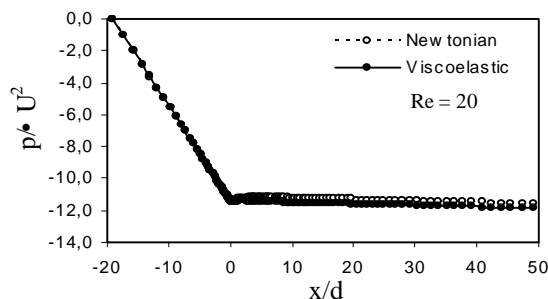


Fig. 11 – Pressure profiles along central plane

## 5. CONCLUSIONS

The planar 1:4 expansion flow of a FENE-MCR model fluid has been simulated by using the finite volume method on a non-uniform grid system and by adopting the CUBISTA scheme to discretize the convection fluxes in the flow and constitutive equations, where the stress tensor can be decomposed into Newtonian and non-Newtonian parts. In this work we only dealt with low Reynolds numbers in the range 0.01 – 20. At low Reynolds number and low expansion ratio (1:4), the flow is almost symmetric in respect to the center plane. Hence we see that the values of the length and intensity of the vortices are the same in the upper and lower sides of the expansion geometry, for range values of Weissenberg and Reynolds numbers. We can also see from results for the Newtonian fluid that for Reynolds numbers larger than 1 inertial forces prevail in the flow, while for Reynolds numbers significantly less than 1 the viscous forces dominate. On the other hand, we see that when  $We$  is large, viscoelastic effects are important in the flow and it is necessary to select a viscoelastic constitutive equation. The present results showing a significant reduction in vortex size and intensity with viscoelasticity could not have been obtained with a generalised Newtonian fluid because here the shear viscosity was kept constant.

## References

- [1] D.V. Boger, K. Walters, Rheological Phenomena in Focus, Rheology Series, vol.4, Elsevier, 1993.
- [2] P.J. Oliveira, Asymmetric flows of viscoelastic fluids in symmetric planar expansion geometries, J. Non-Newtonian Fluid Mechanics. 114 (2003) 33-63.
- [3] D. Drikakis, Bifurcation phenomena in incompressible sudden expansion flows, Phys. Fluids 9 (1997) 76-86.
- [4] R.B. Bird, C.F. Curtiss, R.C. Armstrong, O. Hassager, Dynamics of Polymeric Liquids, vol.2, Kinetic Theory, Wiley, New York, 1977.
- [5] M.D. Chilcott, J.M. Rallison, Creeping flow dilute polymer solutions past cylinders and spheres, J. Non-Newtonian Fluid Mech. 29 (1988) 381-432.
- [6] P.J. Oliveira, F.T. Pinho, G.A. Pinto, Numerical simulation of non-linear elastic flows with a general collocated finite-volume method, J. Non-Newtonian Fluid Mech. 79 (1998) 1-43.
- [7] M.A. Alves, P.J. Oliveira, F.T. Pinho, A convergent and universally bounded interpolation scheme for the treatment of advection, Int. J. Numer. Methods Fluids 41 (2003) 47-75.
- [8] P.S. Scott, F.A. Mirza, J. Vlachopoulos, A finite element analysis of laminar flows through planar and axisymmetric abrupt expansions, Computers & Fluids, Vol. 14, No. 4 (1986) 423-432.